DOI: 10.1002/ejic.201100960

Diverse Coordination Behaviour of Phosphorus(V)-Functionalised 6-Chloroaminobenzothiazole Anions at Various Metal Centres

Simon J. Coles,[a] Sophie H. Dale,[b] Mark R. J. Elsegood,[b] Kirsty G. Gaw,[b] Thomas Gelbrich,[a] Michael B. Hursthouse,[a] Mark E. Light,[a] Thomas A. Noble,[b] and Martin B. Smith*[b]

Keywords: Benzothiazole / Chalcogenides / Phosphanes / Potassium / Structure elucidation

Aminobenzothiazole-functionalised phosphane **1** and its corresponding phosphorus(V) analogues **2**–**4** were synthesised in high yields. New 1D polymeric salts $K[ClC_6H_3NC(S)NP(E)Ph_2]_\infty$ (E = O **5**; E = S **6**) were shown, by using single-crystal X-ray diffraction, to exhibit unique potassium metal ion coordination through either κ^3-N_2O tridentate (E = O) or κ^2-N_2 bridging (E = S) modes. In contrast, κ^2-NE chelation (E = S, Se) was observed upon complexation to a range of metal fragments including {Ir(η^5-Cp*)Cl} (E = S **8**; E = Se **9**), {Rh(η^5-Cp*)Cl} (E = S **10**; E = Se **11**), {Ru(η^6-*p*-MeC_6H_4*i*Pr)Cl} (E = S **12**), {Ru(η^6-C_6Me_6)Cl} (E = S **13**) and {Pt(PMe_2Ph)Cl} (E = S **14**). All new compounds were characterised by a combination of multinuclear NMR, FTIR and microanalysis. Seven compounds were structurally characterised by using single-crystal X-ray crystallography.

Introduction

Chelating anionic ligands, such as the ubiquitous acac anion (acac = acetylacetonato), have attracted considerable interest over the years for their importance in many diverse aspects of coordination chemistry. Aside from acac, many other bidentate anionic ligands bearing group 15 or 16 donor atoms have been widely documented. Scheme 1 illustrates a selection of popular recent examples including: amidinate (**I**),[1] guanidinate (**II**),[2] β-diketiminate (nacnac$^-$) (**III**),[3] bis(phosphinimino)methanide (**IV**)[4] and imidodiphosphinate (**V**)[5] ligands (R and R′ denote various alkyl/silyl/aryl groups; E = O, S, Se, Te). In these examples, the principal bonding motifs observed are either κ^2-NN- or κ^2-EE-chelation. Considerable recent interest in sulfur and selenium analogues of **V** strides from observations that these complexes are suitable single-source precursors for binary metal sulfide[5c] or selenide[5d] thin semiconducting films.

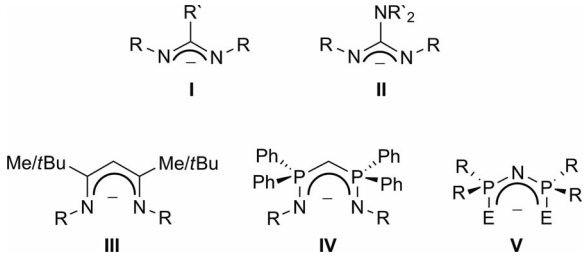

Scheme 1.

As part of continuing studies in our group investigating neutral and singly/doubly deprotonated functionalised tertiary phosphanes,[6] we report here the facile synthesis and structural characterisation of two unusual potassium salts of an anionic, benzothiazole-modified amino(phosphane) oxide and sulfide.[7] We show, depending on the group 16 donor atom (O or S), two distinct coordination modes utilising a combination of both nitrogen and/or O donor centres. Furthermore, classical κ^2-NE-chelation (E = S, Se) was achieved upon facile complexation to a range of late transition metal fragments including {M(η^5-Cp*)Cl} (M = Ir, Rh; Cp* = pentamethylcyclopentadienyl), {Ru(η^6-*p*-MeC_6H_4*i*Pr)Cl}, {Ru(η^6-C_6Me_6)Cl} and {Pt(PMe_2Ph)Cl}. All new compounds reported here were characterised by a combination of spectroscopic and crystallographic techniques.

Results and Discussion

Reaction of commercially available 6-chloroaminobenzothiazole with Ph_2PCl and NEt_3, in diethyl ether, gave, after work-up, amino(phosphane) **1** in excellent (95%) yield.[8] Under standard conditions,[7b] oxidation with either aqueous H_2O_2 (30% w/w), elemental S_8 or grey Se afforded the corresponding phosphorus(V) compounds **2**–**4** in approximately 90% yield. The molecular structure of phosphane oxide **2** was determined (Figure 1) and shows a tautomeric

[a] EPSRC National Crystallography Service, School of Chemistry, University of Southampton, Highfield, Southampton SO17 1BJ, U.K.
[b] Department of Chemistry, Loughborough University, Loughborough, Leics LE11 3TU, U.K.
Fax: +44-1509-223925
E-mail: m.b.smith@lboro.ac.uk

Supporting information for this article is available on the WWW under http://dx.doi.org/10.1002/ejic.201100960.

arrangement with the NH hydrogen on the endocyclic N(2) atom. The P(1)–N(1) [1.636(2) Å], N(1)–C(1) [1.293(3) Å] and C(1)–N(2) [1.353(3) Å] bond lengths provide evidence of delocalisation in the P(1)–N(1)–C(1)–N(2) backbone.[7b] Intermolecular N–H···O H-bonding links molecules of **2** into a 1D polymeric chain [N(2)···O(1A) 2.696(3) Å; N(2)–H(2)···O(1A) 153(3)°].

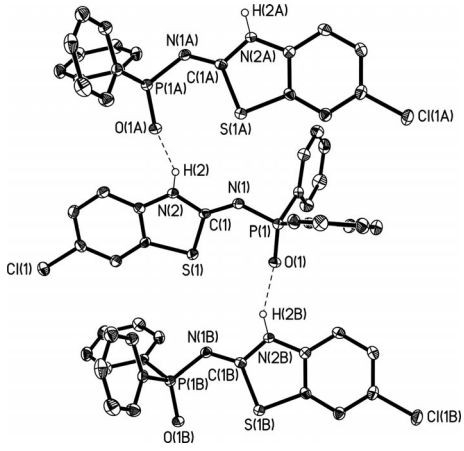

Figure 1. Ellipsoid plot of **2**. Thermal ellipsoids are drawn at the 50% probability level. All hydrogen atoms except those on N(2), N(2A) and N(2B) are omitted for clarity. Selected bond lengths [Å] and angles [°]: P(1)–O(1) 1.4935(18), P(1)–N(1) 1.636(2), N(1)–C(1) 1.293(3), C(1)–N(2) 1.353(3), C(1)–S(1) 1.790(2); O(1)–P(1)–N(1) 117.09(10), P(1)–N(1)–C(1) 125.01(18), N(1)–C(1)–N(2) 122.6(2), N(1)–C(1)–S(1) 128.10(19). Symmetry operator: A = $x + 1/2, -y + 1/2, -z + 1$.

Metallation of **2**–**4** was smoothly achieved, at ambient temperature, with *t*BuOK in MeOH to generate potassium salts **5**–**7**. Cleavage of the chloride bridge[9] of $[MCl(\mu\text{-}Cl)(\eta^5\text{-}Cp^*)]_2$ (M = Ir, Rh), $[RuCl(\mu\text{-}Cl)(\eta^6\text{-}p\text{-}MeC_6H_4\text{-}iPr)]_2$, $[RuCl(\mu\text{-}Cl)(\eta^6\text{-}C_6Me_6)]_2$ or $[PtCl(\mu\text{-}Cl)(PMe_2Ph)]_2$ with 2 equiv. of **6** or **7** (preformed or generated directly from **3** or **4**/*t*BuOK) gave the neutral mononuclear metal complexes $Ir(\eta^5\text{-}Cp^*)Cl$(**6**/**7**) (E = S **8**; E = Se **9**), $Rh(\eta^5\text{-}Cp^*)Cl$(**6**/**7**) (E = S **10**; E = Se **11**), $Ru(\eta^6\text{-}p\text{-}MeC_6H_4iPr)Cl$(**6**) (**12**), $Ru(\eta^6\text{-}p\text{-}C_6Me_6)Cl$(**6**) (**13**) and $Pt(PMe_2Ph)Cl$(**6**) (**14**) in good yields (Scheme 2).

The molecular structures of potassium salts **5** and **6** were successfully determined by using X-ray crystallography (Figures 2 and 3). For oxide **5**, the asymmetric unit comprises two potassium cations, two anionic ligands and half a chloroform molecule of crystallisation, the latter disordered over an inversion centre. The unsaturated nitrogen and oxygen atoms of the anionic ligand bridge two potassium centres, which leads to a centrosymmetric dimer comprising two $K_2N_2O_2$ units. In contrast, the second N atom bridges[7b] to an adjacent potassium ion within a second dinuclear unit. The K(1)–N(2′A)/K(1)–N(2′) bond lengths are 3.057(3)/3.103(3) Å with K(1)–O(1′A)/K(1)–O(1′) bond lengths of 2.623(2)/2.871(2) Å; both are in the normal expected range. Within the 6-chloroaminobenzothiazole anion, the P(1)–O(1), P(1)–N(1), N(1)–C(1), C(1)–N(2), C(1)–S(1) bond lengths are 1.494(2), 1.621(2), 1.341(4), 1.310(4), 1.782(3) Å, respectively, and a more pronounced

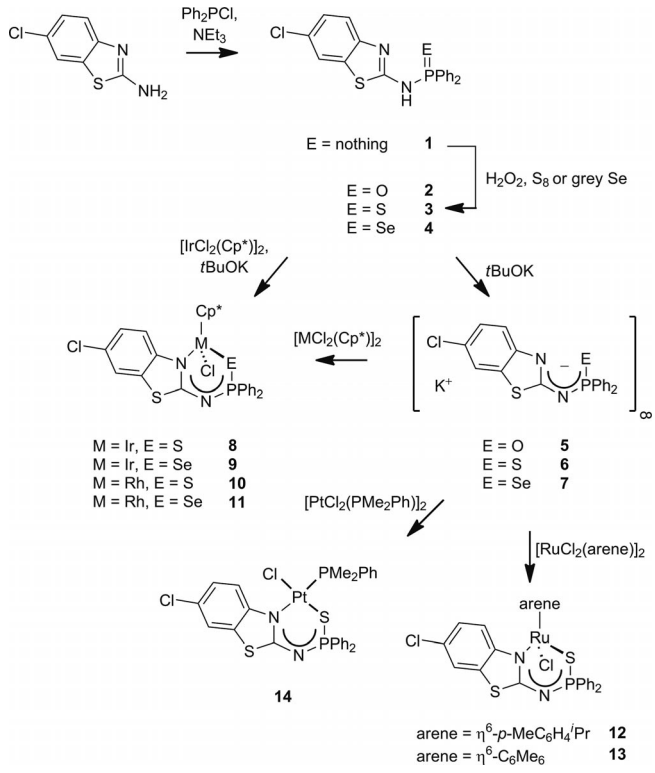

Scheme 2. Synthesis of compounds **1**–**14**.

N(1)–C(1)–N(2) bond angle of 129.9(3)° (with respect to sulfide **6**, vide infra) was observed.[10] These metric parameters suggest some degree of delocalisation within the O(1)–P(1)–N(1)–C(1)–N(2) skeletal backbone. The coordination environment around K(1) is completed by a further K(1)–N(1) bond [2.820(2) Å] from an adjacent dimeric unit and additional K···π contacts [K(1)···C(14) 3.447(3) Å; K(1)···C(19′) 3.274(4) Å; K(1)···C(19) 3.339(3) Å]. Further intermolecular contacts are present within the second unique dimeric unit and comprise K···C [3.392(4) Å] and K···S [3.6260(11) Å]. These are significantly shorter than the van der Waals radii for K/C (ca. 4.5 Å) and K/S (ca. 4.5 Å) atoms.[11]

In contrast to **5**, different structural ligating features are clearly evident for the solvated sulfide analogue **6**. Each potassium is sevenfold coordinated by four nitrogen atoms of the deprotonated 6-chloroaminobenzothiazole ligands and three MeOH molecules. Moreover, the unsaturated/terminal amido N atoms of both anionic ligands bridge between two symmetry-equivalent K metal ions. The resulting dimer is centrosymmetric and has a K_2N_4 unit at its centre. Imposed by symmetry, each four-membered K_2N_2 ring is exactly planar. The rings exhibit K–N bond lengths of 2.865(2) and 2.920(2) Å, with additional longer K–N distances of 3.138(2) and 3.054(2) Å.[12] The two K_2N_2 rings form a dihedral angle of 58.83(5)°. Within the anionic ligand the N(1)–C(7) and N(2)–C(7) bond lengths are 1.322(3) and 1.334(3) Å, respectively, indicative of delocalisation within the N–C–N backbone. The P(1)–N(2), P(1)–S(2) and S(1)–C(7) distances are 1.627(2), 1.9847(9) and 1.799(2) Å,

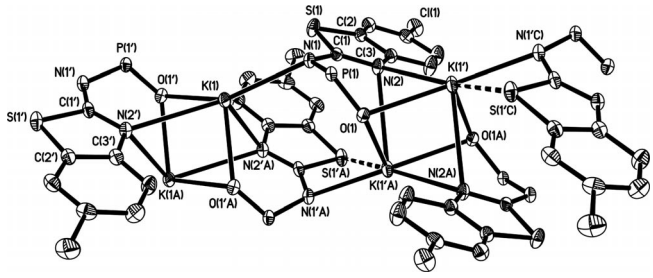

Figure 2. Ellipsoid plot of **5** showing the coordination environment around each potassium metal centre. Thermal ellipsoids are drawn at the 30% probability level. All C–*H* hydrogen atoms and phenyl groups on phosphorus are omitted for clarity. Selected bond lengths [Å] and angles [°]: K(1)–N(1) 2.820(2), K(1)–N(2′A) 3.057(3), K(1)–N(2′) 3.103(3), K(1)–O(1′A) 2.623(2), K(1)–O(1′) 2.871(2), P(1)–O(1) 1.494(2), P(1)–N(1) 1.621(2), N(1)–C(1) 1.341(4), C(1)–N(2) 1.310(4), C(1)–S(1) 1.782(3); O(1)–P(1)–N(1) 120.34(13), P(1)–N(1)–C(1) 119.6(2), N(1)–C(1)–N(2) 129.9(3). Symmetry operators: $-x + 2, -y, -z + 1$; $-x + 2, -y, -z + 2$; x, *y*, *z* + 1.

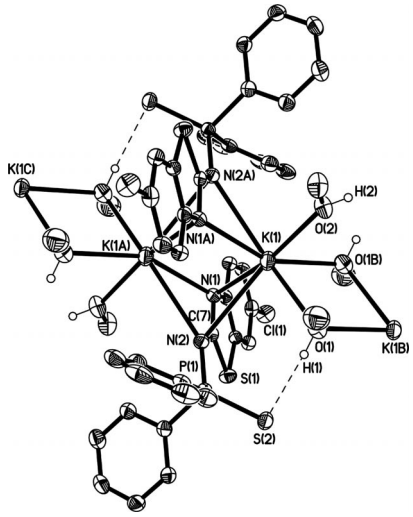

Figure 3. Ellipsoid plot of **6** showing part of the 1D chain and the coordination environment around K(1). Thermal ellipsoids are drawn at the 50% probability level. All C–H hydrogen atoms except those on O(1), O(1A) and O(2) are omitted for clarity. Selected bond lengths [Å] and angles [°]: K(1)–N(1) 2.920(2), K(1)–N(2) 3.138(2), K(1)–N(1A) 2.865(2), K(1)–N(2A) 3.054(2), K(1)–O(1) 2.829(2), K(1)–O(2) 2.6882(19), K(1)–O(1A) 2.779(2), N(1)–C(7) 1.322(3), N(2)–C(7) 1.334(3), S(1)–C(7) 1.799(2), N(2)–P(1) 1.627(2), P(1)–S(2) 1.9851(9); N(1)–K(1)–N(2) 44.93(5), K(1)–N(2)–C(7) 81.41(13), N(1)–C(7)–N(2) 122.1(2), C(7)–N(1)–K(1) 90.68(14), P(1)–N(2)–C(7) 123.61(18), K(1)–N(2)–P(1) 125.08(10), N(2)–P(1)–S(2) 117.84(7). Symmetry operators: $-x, -y, -z - 1$; $-x + 1, -y, -z - 1$; $1 + x, y, z$.

respectively.[10,13] The potassium ion is additionally coordinated by two bridging [K–O 2.779(2) and 2.829(2) Å] and one nonbridging MeOH [K–O 2.6882(19) Å] solvent molecules.[14] As a result, the dimeric units are connected through K_2O_2 rings to give 1D chains that extend parallel to the crystallographic *a* axis. The plane of the K_2O_2 core forms dihedral angles of 59.70(8) and 68.26(8)° with adjacent K_2N_2 rings. Furthermore, the K···K separations are 3.6938(10) and 4.2659(11) Å within the K_2N_2 and K_2O_2 units, respectively. The coordination polyhedron about potassium is a capped trigonal prism in which the four nitrogen substituents are exactly planar. There are also two intermolecular O–H···S hydrogen bonds, which presumably assist in stabilisation of the unusual 1D chain [O(1)···S(2) 3.247(2) Å; O(1)–H(1)···S(2) 169(3)° and O(2)···S(2) 3.263(2) Å; O(2)–H(2)···S(2) 154(2)°; see Figure 3 and Supporting Information].

The molecular structures of **8** (Supporting Information), **9** and **11** (Figures 4 and 5) are isostructural (Tables 1 and 2) and each reveals a classic piano-stool arrangement comprising an η^5-Cp*, a chelating κ^2-N/Se-[$ClC_6H_3NC(S)NP(E)Ph_2$]$^-$ (E = S, Se) anion and a chloride ligand around

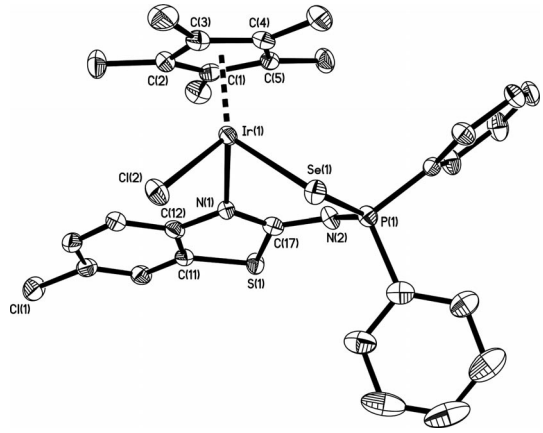

Figure 4. Ellipsoid plot of **9**. Thermal ellipsoids are drawn at the 50% probability level. All hydrogen atoms are removed for clarity. Selected bond lengths [Å] and angles [°]: Ir(1)–Se(1) 2.5102(4), Ir(1)–N(1) 2.128(3), Ir(1)–Cl(2) 2.4161(9), Ir(1)–C_{av} 2.166(4), Se(1)–P(1) 2.1591(10), P(1)–N(2) 1.610(3), N(2)–C(17) 1.324(4), N(1)–C(17) 1.335(4); Cl(2)–Ir(1)–N(1) 91.24(8), Cl(2)–Ir(1)–Se(1) 82.14(2), N(1)–Ir(1)–Se(1) 88.93(7), Ir(1)–Se(1)–P(1) 97.57(3), Se(1)–P(1)–N(2) 117.07(12), P(1)–N(2)–C(17) 125.9(3), N(1)–C(17)–N(2) 130.9(3), Ir(1)–N(1)–C(17) 122.6(2).

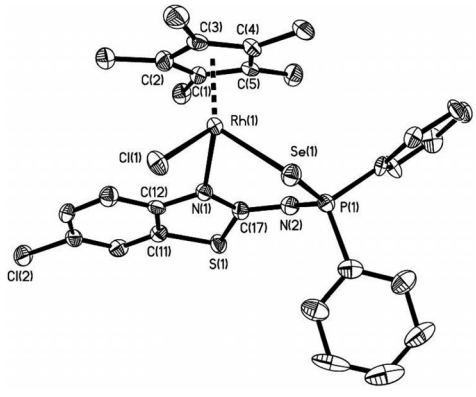

Figure 5. Ellipsoid plot of **11**. Thermal ellipsoids are drawn at the 50% probability level. All hydrogen atoms are removed for clarity. Selected bond lengths [Å] and angles [°]: Rh(1)–Se(1) 2.5110(7), Rh(1)–N(1) 2.132(5), Rh(1)–Cl(1) 2.4217(16), Rh(1)–C_{av} 2.167(6), Se(1)–P(1) 2.1584(17), P(1)–N(2) 1.606(5), N(2)–C(17) 1.332(8), N(1)–C(17) 1.338(7); Cl(1)–Rh(1)–N(1) 93.40(13), Cl(1)–Rh(1)–Se(1) 83.26(4), N(1)–Rh(1)–Se(1) 89.69(12), Rh(1)–Se(1)–P(1) 97.30(5), Se(1)–P(1)–N(2) 117.9(2), P(1)–N(2)–C(17) 126.1(4), N(1)–C(17)–N(2) 129.8(5), Rh(1)–N(1)–C(17) 123.4(4).

the metal centre. Extensive delocalisation within the M(1)–E(1)–P(1)–N(2)–C(17)–N(1) (M = Ir, Rh) six-membered ring is evident, as indicated by the appropriate differences in bond lengths. Hence the P–Se bond lengths [2.1591(10) Å for **9**; 2.1584(17) Å for **11**] are intermediate between those expected for P–Se single and P=Se double bonds, which is supportive of regular charge delocalisation across the $SePCN_2$ framework.[15] The six-membered metallacyclic ring in **8**, **9** and **11** adopts an asymmetric boat conformation in which atoms N(1), C(17), P(1) and E(1) are essentially coplanar to within approximately ±0.04 Å and N(2) and Ir(1) lie in the range 0.244–0.256 and 1.121–1.250 Å, respectively, to the same side of this plane.

The molecular structure of **14** (Figure 6) confirms the κ^2-N/S-bidentate behaviour of the $[ClC_6H_3NC(S)NP(S)Ph_2]^-$ anion around the square-planar Pt^{II} centre with PMe_2Ph/Cl^- present as auxiliary ligands. Of the two possible geometric isomers that could be anticipated, the X-ray structure of **14** reveals that the N(1) donor centre is *trans* to P(2). The Pt(1)–P(2), Pt(1)–S(1), Pt(1)–N(1) and Pt(1)–Cl(1) bond

Table 1. Crystallographic data for **2**, **5**, **6** and **8**.

Compound	**2**	**5**	**6**	**8**
Empirical formula	$C_{19}H_{14}ClN_2OPS$	$2(C_{38}H_{26}Cl_2K_2N_4O_2P_2S_2)\cdot CHCl_3$	$C_{21}H_{21}ClKN_2O_2PS_2$	$C_{29}H_{28}Cl_2IrN_2PS_2$
Formula weight	384.80	1810.98	503.04	762.72
Crystal system	orthorhombic	triclinic	triclinic	monoclinic
Space group	$P2_12_12_1$	$P\bar{1}$	$P\bar{1}$	$P2_1/n$
a [Å]	10.6308(2)	13.1740(2)	7.7261(2)	7.9797(16)
b [Å]	12.0146(4)	13.2239(2)	12.8359(3)	16.183(3)
c [Å]	13.7050(4)	13.6498(2)	13.0946(4)	21.534(4)
α [°]		107.8897(10)	68.9510(10)	
β [°]		113.0629(8)	80.0470(10)	90.41(3)
γ [°]		91.7783(8)	77.472(2)	
Volume [Å^3]	1750.47(8)	2050.76(5)	1176.66(5)	2780.7(9)
Z	4	1	2	4
T [K]	120(2)	150(2)	150(2)	150(2)
Density (calcd.) [Mg/m^3]	1.460	1.466	1.420	1.822
Absorption coeff. [mm^{-1}]	0.438	0.679	0.605	5.224
Crystal habit, colour	block, colourless	plate, colourless	block, colourless	needle, yellow
Crystal size [mm^3]	0.18 × 0.10 × 0.08	0.17 × 0.17 × 0.10	0.10 × 0.07 × 0.05	0.32 × 0.04 × 0.04
θ Range [°]	3.39–27.54	3.10–25.25	2.95–25.25	2.99–27.49
Independent reflections	4013	7398	4250	6368
R_{int}	0.0767	0.0433	0.0479	0.0523
Final *R*, *Rw*[a]	0.0406, 0.0845	0.0491, 0.1372	0.0394, 0.0978	0.0303, 0.0650

[a] $R = \Sigma||F_o| - |F_c||/\Sigma|F_o|$ for "observed" reflections having $F2 > 2\sigma(F2)$. $Rw = [\Sigma w(F_o^2 - F_c^2)^2/\Sigma w(F_o^2)^2]^{1/2}$ for all data.

Table 2. Crystallographic data for **9**, **11** and **14**.

Compound	**9**	**11**	**14**
Empirical formula	$C_{29}H_{28}Cl_2IrN_2PSSe$	$C_{29}H_{28}Cl_2N_2PRhSSe$	$C_{27}H_{24}Cl_2N_2P_2PtS_2\cdot 0.91OEt_2\cdot 0.09CH_2Cl_2$
Formula weight	809.62	720.33	843.62
Crystal system	monoclinic	monoclinic	monoclinic
Space group	$P2_1/n$	$P2_1/n$	$P2_1/n$
a [Å]	8.00540(10)	7.9701(3)	9.7390(19)
b [Å]	16.2441(3)	16.3122(8)	15.142(3)
c [Å]	21.5752(5)	21.5858(13)	23.176(5)
α [°]			
β [°]	90.4909(7)	90.811(2)	97.93(3)
γ [°]			
Volume [Å^3]	2805.55(9)	2806.1(2)	3385.0(12)
Z	4	4	4
T [K]	150(2)	120(2)	150(2)
Density (calcd.) [Mg/m^3]	1.917	1.705	1.655
Absorption coeff. [mm^{-1}]	6.401	2.251	4.561
Crystal habit, colour	block, orange	plate, orange	block, colourless
Crystal size [mm^3]	0.15 × 0.10 × 0.08	0.12 × 0.08 × 0.01	0.15 × 0.15 × 0.10
θ Range [°]	3.00–26.00	2.99–25.33	2.98–27.46
Independent reflections	5498	5083	7582
R_{int}	0.0398	0.129	0.0471
Final *R*, *Rw*[a]	0.0263, 0.0554	0.0530, 0.1067	0.0360, 0.0826

[a] $R = \Sigma||F_o| - |F_c||/\Sigma|F_o|$ for "observed" reflections having $F2 > 2\sigma(F2)$. $Rw = [\Sigma w(F_o^2 - F_c^2)^2/\Sigma w(F_o^2)^2]^{1/2}$ for all data.

lengths are broadly as anticipated, and the S(1)–P(1)–N(2)–C(1)–N(1) distances are similar to those found in **8** (Supporting Information).

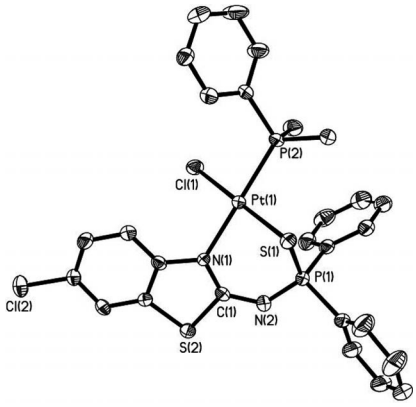

Figure 6. Ellipsoid plot of **14**. Thermal ellipsoids are drawn at the 50% probability level. All hydrogen atoms are removed for clarity. Selected bond lengths [Å] and angles [°]: Pt(1)–S(1) 2.3177(11), Pt(1)–N(1) 2.107(3), Pt(1)–Cl(1) 2.3076(11), Pt(1)–P(2) 2.2336(11), S(1)–P(1) 2.0251(17), P(1)–N(2) 1.599(4), N(2)–C(1) 1.335(5), C(1)–N(1) 1.338(5); Cl(1)–Pt(1)–N(1) 90.07(9), Cl(1)–Pt(1)–S(1) 177.78(4), N(1)–Pt(1)–S(1) 89.82(9), Pt(1)–S(1)–P(1) 89.84(5), S(1)–P(1)–N(2) 116.94(15), P(1)–N(2)–C(1) 125.3(3), N(2)–C(1)–N(1) 129.1(4), Pt(1)–N(1)–C(1) 121.6(3).

Conclusions

We observed three distinct ligating modes for a derivatised benzothiazole anion at a potassium or late transition metal centre based on Ir^{III}, Rh^{III}, Ru^{II} or Pt^{II}. Further studies are underway and will be reported in due course.

Experimental Section

Materials: The syntheses of compounds **1**–**4** were conducted under a nitrogen atmosphere whilst all other reactions were carried out under aerobic conditions. Dichloromethane was previously distilled from CaH_2, diethyl ether from sodium/benzophenone, thf and hexanes from sodium. The chlorido-bridged dimers $[IrCl(\mu\text{-}Cl)(\eta^5\text{-}Cp^*)]_2$,[16] $[RhCl(\mu\text{-}Cl)(\eta^5\text{-}Cp^*)]_2$,[16] $[RuCl(\mu\text{-}Cl)(\eta^6\text{-}p\text{-}MeC_6H_4iPr)]_2$,[17] $[RuCl(\mu\text{-}Cl)(\eta^6\text{-}C_6Me_6)]_2$[18] and $[PtCl(\mu\text{-}Cl)(PMe_2Ph)]_2$[19] were synthesised according to published methods. All other solvents and chemicals were obtained from commercial suppliers. With the exception of Ph_2PCl, which was distilled under high vacuum prior to use, all other solvents and chemicals were used without any further purification.

Instrumentation: Fourier transform infrared (FTIR) spectra were recorded within pressed KBr pellets by using either a Perkin–Elmer system 2000 (over the range 4000–400 cm^{-1}) or Spectrum 100S (over the range 4000–250 cm^{-1}) Fourier-transform spectrometer. ^1H NMR and $^{31}P\{^1H\}$ NMR spectra were recorded with a JEOL FX90Q, Bruker AC250 FT, Bruker FX 400 or Bruker DPX-400 FT spectrometer with chemical shifts (δ) reported relative to either external tetramethylsilane (TMS) or 85% H_3PO_4. Coupling constants (J) were recorded in Hertz. All NMR spectra were recorded in $CDCl_3$ unless otherwise stated. Elemental analyses (Perkin–Elmer 2400 or Exeter Analytical Inc. CE-440 CHN Elemental Analysers) were performed by the Loughborough University Analytical Services within the Department of Chemistry. The mass spectra for **1**, **2**, **4** and **12**–**14** were analysed (JEOL SX102 instrument) by fast atom bombardment (FAB) in a positive ionisation mode by using a 3-nitrobenzyl alcohol (NOBA) matrix. Compounds **3**, **5**, **6**, **8** and **9** were analysed (Thermofisher LTQ Orbitrap XL) by nano-electrospray (nano-ESI) in a positive ionisation mode with CH_2Cl_2/CH_3OH as solvent and $NH_4[OAc]$.

Compound 1: To a stirred solution of 6-chloroaminobenzothiazole (4.181 g, 22.64 mmol) and NEt_3 (2.507 g, 24.78 mmol) in diethyl ether (50 mL) at 0 °C was added dropwise a solution of Ph_2PCl (4.948 g, 22.43 mmol) over 30 min. The resulting white suspension was stirred for 18 h and concentrated to dryness, and degassed distilled water (50 mL) was added. Solid **1** was collected by suction filtration, washed with distilled water (50 mL), *n*-hexane (50 mL), absolute ethanol (2 × 30 mL) and dried in vacuo. Yield: 7.986 g (95%). $^{31}P\{^1H\}$ NMR ($CDCl_3$): δ = 42.5 ppm. ^1H NMR: δ = 7.50 (s, arom. H), 7.41–7.29 (m, arom. H), 7.20 (s, arom. H), 7.08 (s, arom. H) ppm. FTIR: $\tilde{\nu}$ = 3113 (NH), 1594 (CN), 924 (PN) cm^{-1}. FAB-MS: m/z = 369 $[M]^+$. $C_{19}H_{14}ClN_2PS$ (368.8): calcd. C 61.88, H 3.83, N 7.60; found C 61.52, H 3.80, N 7.54.

Compound 2: To a stirred solution of **1** (0.192 g, 0.517 mmol) in thf (10 mL) was added aqueous H_2O_2 (30% w/w, 0.1 mL, 0.88 mmol). The solution was stirred for approximately 1 h, the volume was reduced to approximately 5 mL, and diethyl ether (30 mL) was added. The solid was collected by suction filtration, washed with diethyl ether (5 mL) and dried in vacuo. Yield: 0.193 g (97%). $^{31}P\{^1H\}$ NMR ($CDCl_3$): δ = 26.5 ppm. ^1H NMR: δ = 7.82–7.77 (m, arom. H), 7.47–7.30 (arom. H), 7.14 (dd, J = 8.6, J = 2 Hz, arom. H), 7.04 (d, J = 8.6 Hz, arom. H) ppm. FTIR: $\tilde{\nu}$ = 3076 (NH), 1631 (CN), 1163 (PO), 957 (PN) cm^{-1}. FAB-MS: m/z = 385 $[M]^+$. $C_{19}H_{14}ClN_2OPS$ (384.8): calcd. C 59.30, H 3.67, N 7.28; found C 59.25, H 3.63, N 7.12.

Compound 3: The solids **1** (1.000 g, 2.696 mmol) and S_8 (0.086 g, 2.682 mmol) were stirred in thf (20 mL) for 4 h. The solvent was concentrated in vacuo to approximately 1–2 mL, and addition of diethyl ether (30 mL) resulted in a pale yellow solid **3**. The product was collected by suction filtration, washed with diethyl ether (5 mL) and dried in vacuo. Yield: 1.028 g (95%). $^{31}P\{^1H\}$ NMR ($CDCl_3$): δ = 49.5 ppm. ^1H NMR: δ = 8.01–7.87 (m, arom. H), 7.41–7.33 (arom. H), 7.17 (dd, J = 8.6, J = 2 Hz, arom. H), 7.01 (d, J = 8.6 Hz, arom. H) ppm. FTIR: $\tilde{\nu}$ = 3181 (NH), 1624 (CN), 948 (PN), 626 (PS) cm^{-1}. FAB-MS: m/z = 401 $[M]^+$. $C_{19}H_{14}ClN_2PS_2$ (400.9): calcd. C 56.93, H 3.52, N 6.99; found C 56.92, H 3.61, N 6.84.

Compound 4: The solids **1** (0.165 g, 0.445 mmol) and grey Se (0.036 g, 0.456 mmol) were stirred in thf (20 mL) for 4 h. Unreacted Se was removed by filtration through a Celite pad. The solvent was concentrated in vacuo to approximately 1–2 mL, and addition of diethyl ether (30 mL) resulted in a colourless solid **4**. The product was collected by suction filtration, washed with diethyl ether (5 mL) and dried in vacuo. Yield: 0.175 g (88%). $^{31}P\{^1H\}$ NMR [$CDCl_3$/$(CD_3)_2SO$]: δ = 43.9 ($^1J_{PSe}$ = 726 Hz) ppm. ^1H NMR: δ = 7.92–7.87 (m, arom. H), 7.37–7.35 (arom. H), 7.18 (dd, J = 8.5, J = 2 Hz, arom. H), 7.02 (d, J = 8.5 Hz, arom. H) ppm. FTIR: $\tilde{\nu}$ = 3070 (NH), 1619 (CN), 948 (PN), 586 (PSe) cm^{-1}. FAB-MS: m/z = 449 $[M]^+$. $C_{19}H_{14}ClN_2PSSe$ (447.8): calcd. C 50.96, H 3.15, N 6.26; found C 51.11, H 2.94, N, 6.12.

Potassium Salts 5–7: An illustrative example is given here for the synthesis of compound **5**. To a suspension of **2** (0.100 g, 0.260 mmol) in MeOH (10 mL) was added *t*BuOK (0.029 g, 0.258 mmol). The solution was stirred for 18 h and concentrated to

dryness to afford the moisture-sensitive solid **5**. Yield: 0.087 g (65%). Selected data for **5**: $^{31}P\{^1H\}$ NMR (CD_3OD): δ = 23.8 ppm. ^1H NMR (CD_3OD): δ = 7.91–7.07 (arom. H) ppm. FTIR: $\tilde{\nu}$ = 1220 (PO), 965 (PN) cm^{-1}. FAB-MS: *m/z* = 385 $[M - K + 2H]^+$. $C_{19}H_{13}ClKN_2OPS{\cdot}0.5CHCl_3$ (482.6): calcd. C 48.53, H 2.83, N 5.81; found C 49.17, H 2.70, N 5.47. The sulfide analogue **6** was prepared in 67% yield. Selected data for **6**: $^{31}P\{^1H\}$ NMR (CD_3OD): δ = 47.4 ppm. ^1H NMR: δ = 8.05–7.02 (arom. H) ppm. FTIR: $\tilde{\nu}$ = 962 (PN), 610 (PS) cm^{-1}. FAB-MS: *m/z* = 401 $[M - K(CH_3OH)_2]^+$. $C_{19}H_{13}ClKN_2PS_2{\cdot}2H_2O$ (475.0): calcd. C 48.04, H 3.61, N 5.90; found C 47.49, H 3.50, N 5.48. The selenide analogue **7** was similarly prepared in quantitative yield from **4**. Selected data for **7**: $^{31}P\{^1H\}$ NMR [$(CD_3)_2SO$]: δ = 33.3 ($^1J_{PSe}$ = 697 Hz) ppm. ^1H NMR: δ = 7.95–7.05 (arom. H) ppm. $C_{19}H_{13}ClKN_2PSSe{\cdot}4H_2O$ (557.9): calcd. C 40.90, H 3.80, N 5.02; found C 40.61, H 2.39, N 4.57.

Complexes 8–14: An illustrative example is given here for the synthesis of compound **9**. To an orange suspension of $[IrCl(\mu\text{-}Cl)(\eta^5\text{-}Cp^*)]_2$ (0.058 g, 0.073 mmol) in thf (10 mL) were added **4** (0.065 g, 0.145 mmol) and *t*BuOK (0.017 g, 0.151 mmol). The orange solution was stirred at room temp. for approximately 3 h and concentrated to dryness under reduced pressure. The residue was extracted into CH_2Cl_2 (10 mL), filtered through a Celite plug and concentrated to approximately 1 mL. Addition of diethyl ether (20 mL) afforded a yellow solid, which was collected by suction filtration and dried in vacuo. Yield: 0.098 g (80%). Selected data for **9**: $^{31}P\{^1H\}$ NMR ($CDCl_3$): δ = 11.9 ($^1J_{PSe}$ = 554 Hz) ppm. ^1H NMR: δ = 8.22 (d, *J* = 8.8 Hz, arom. H), 8.10 (m, arom. H), 7.66 (m, arom. H), 7.45 (m, arom. H), 7.29 (d, *J* = 2.4 Hz, arom. H), 7.23 (m, arom. H), 7.13 (dd, *J* = 8.8, *J* = 2.1 Hz, arom. H), 1.30 (Cp*) ppm. FTIR: $\tilde{\nu}$ = 1492 (CN), 577 (PSe) cm^{-1}. FAB-MS: *m/z* = 775 $[M - Cl]^+$. $C_{29}H_{28}Cl_2IrN_2PSSe$ (810.4): calcd. C 42.98, H 3.49, N 3.46; found C 42.72, H 3.47, N 3.41. In a similar manner, complex **8** was prepared in 78% yield. Selected data for **8**: $^{31}P\{^1H\}$ NMR ($CDCl_3$): δ = 23.1 ppm. ^1H NMR: δ = 8.13–8.08 (m, arom. H), 7.72 (m, arom. H), 7.46 (m, arom. H), 7.29–7.21 (m, arom. H), 7.12 (dd, *J* = 8.8, *J* = 2.4 Hz, arom. H), 1.30 (Cp*) ppm. FTIR: $\tilde{\nu}$ = 1493 (CN), 601 (PS) cm^{-1}. FAB-MS: *m/z* = 726 $[M - Cl]^+$. $C_{29}H_{28}Cl_2IrN_2PS_2$ (763.5): calcd. C 45.62, H 3.70, N 3.67; found C 45.45, H 3.47, N 3.45. Complexes **10**–**14** were prepared from the isolated potassium salts **6** or **7** and the appropriate chloride-bridged dimer (isolated yields given in parentheses): **10** (77%), **11** (56%), **12** (84%), **13** (75%), **14** (60%). Selected data for **10**: $^{31}P\{^1H\}$ NMR ($CDCl_3$): δ = 27.8 ppm. ^1H NMR: δ = 8.31 (d, *J* = 8.8 Hz, arom. H), 8.12 (m, arom. H), 7.71 (m, arom. H), 7.45 (m, arom. H), 7.30 (d, *J* = 2.2 Hz, arom. H), 7.14 (dd, *J* = 8.8, *J* = 2.2 Hz, arom. H), 1.31 (Cp*) ppm. FTIR: $\tilde{\nu}$ = 1494 (CN), 601 (PS) cm^{-1}. $C_{29}H_{28}Cl_2N_2PRhS_2$ (673.5): calcd. C 51.71, H 4.20, N 4.16; found C 51.43, H 4.17, N 3.94. Selected data for **11**: $^{31}P\{^1H\}$ NMR ($CDCl_3$): δ = 16.7 ($^1J_{PSe}$ 564 Hz, $^2J_{PRh}$ 3.8 Hz) ppm. ^1H NMR: δ = 8.44 (d, *J* = 8.9 Hz, arom. H), 8.14 (m, arom. H), 7.65 (m, arom. H), 7.46 (m, arom. H), 7.32 (d, *J* = 2.2 Hz, arom. H), 7.16 (dd, *J* = 8.9, *J* = 2.2 Hz, arom. H), 1.32 (Cp*) ppm. FTIR: $\tilde{\nu}$ = 1487 (CN), 576 (PSe) cm^{-1}. $C_{29}H_{28}Cl_2N_2PRhSSe$ (720.26): calcd. C 48.36, H 3.93, N 3.89; found C 48.10, H 3.76, N 3.86. Selected data for **12**: $^{31}P\{^1H\}$ NMR ($CDCl_3$): δ = 31.7 ppm. ^1H NMR: δ = 8.34 (d, *J* = 8.9 Hz, arom. H), 8.28–7.21 (m, arom. H), 7.15 (dd, *J* = 8.9, *J* = 2.2 Hz, arom. H), 5.54 (d, *J* = 5.4 Hz, cym), 5.24 (d, *J* = 6.1 Hz, cym), 5.13 (d, *J* = 5.4 Hz, cym), 4.44 (d, *J* = 5.8 Hz, cym), 2.77 (sept, CH), 2.10 (s, CH_3), 1.50 (Cp*), 1.13 (virtual t, CH_3) ppm. FTIR: $\tilde{\nu}$ = 1493 (CN), 606 (PS) cm^{-1}. FAB-MS: *m/z* = 670 $[M]^+$. $C_{29}H_{27}Cl_2N_2PRuS_2$ (670.7): calcd. C 51.93, H 4.07, N 4.18; found C 52.11, H 4.25, N 3.76. Selected data for **13**: $^{31}P\{^1H\}$ NMR ($CDCl_3$): δ = 27.3 ppm. ^1H NMR: δ = 8.29 (d, *J* = 8.8 Hz, arom. H), 8.11 (m, arom. H), 7.63 (m, arom. H), 7.44 (m, arom. H), 7.29 (d, *J* = 2.3 Hz, arom. H), 7.14 (m, arom. H), 1.76 (s, CH_3) ppm. FTIR: $\tilde{\nu}$ = 1486 (CN), 602 (PS) cm^{-1}. FAB-MS: *m/z* = 698 $[M]^+$. $C_{31}H_{31}Cl_2N_2PRuS_2$ (698.7): calcd. C 53.29, H 4.48, N 4.01; found C 53.17, H 4.33, N 3.83. Selected data for **14**: $^{31}P\{^1H\}$ NMR ($CDCl_3$): δ = –20.3 ($^1J_{PPt}$ = 3385 Hz), 27.1 ($^2J_{PPt}$ = 138 Hz) ppm. ^1H NMR: δ = 7.94 (d, *J* = 8.8 Hz, arom. H), 7.83 (m, arom. H), 7.49–7.27 (m, arom. H), 7.14 (dd, *J* = 8.8, *J* = 2.2 Hz, arom. H), 1.49 (br. s, CH_3) ppm. FTIR: $\tilde{\nu}$ = 1496 (CN), 597 (PS) cm^{-1}. FAB-MS: *m/z* = 767 $[M]^+$. $C_{27}H_{24}Cl_2N_2P_2PtS_2$ (768.6): calcd. C 42.19, H 3.15, N 3.65; found C 42.58, H 3.57, N 3.40.

Single-Crystal X-ray Structure Determinations: Slow diffusion of hexanes into a $CDCl_3$ solution of **2** gave suitable crystals. Vapour diffusion of Et_2O into a $CDCl_3$/MeCN solution of **5** gave suitable crystals. Slow concentration of a MeOH solution of **6** gave suitable crystals. X-ray quality crystals of **8**, **9** and **11** were obtained upon slow diffusion of petroleum ether (b.p. 60–80 °C) into a $CDCl_3$ solution. Vapour diffusion of Et_2O into a $CDCl_3$ solution of **14** gave suitable crystals. Measurements for **2**, **5**, **6**, **8**, **9**, **11** and **14** were obtained with a Nonius κ CCD area-detector diffractometer mounted at the window of a rotating molybdenum anode, and Ω scans were employed such that 95% of the unique data were recorded at least once. Data collection and processing were carried out with the programs COLLECT[20] and DENZO,[21] and an empirical absorption correction was applied with SORTAV.[22] The structures were solved by direct methods or Patterson synthesis[23,24] and refined by full-matrix least-squares[24] on F^2. Non-hydrogen atoms were refined anisotropically, and hydrogen atoms were treated by using a riding model, except for O*H* in **6**, for which coordinates were freely refined. Disordered CH_2Cl_2 (9%) in **14** was isotropically modelled. CCDC-223295 (for **14**), -838885 (for **5**), -838886 (for **6**), -838887 (for **9**), -852752 (for **2**), -852753 (for **8**) and -852754 (for **11**) contain the supplementary crystallographic data for this paper. These data can be obtained free of charge from The Cambridge Crystallographic Data Centre via www.ccdc.cam.ac.uk/data_request/cif.

Supporting Information (see footnote on the first page of this article): Additional X-ray figures for **5**, **6** and **8**.

Acknowledgments

We would like to thank the Engineering and Physical Sciences Research Council (EPSRC) for a studentship (K. G. G.), Infineum UK Ltd for financial support and Johnson Matthey plc for loan of precious metal. The EPSRC mass spectrometry service at Swansea is gratefully acknowledged.

[1] For recent examples of amidinate chemistry, see: a) S. Collins, *Coord. Chem. Rev.* **2011**, *255*, 118–138; b) E. F. Trunkely, A. Epshteyn, P. Y. Zavalij, L. R. Sita, *Organometallics* **2010**, *29*, 6587–6593; c) J. R. Walensky, R. L. Martin, J. W. Ziller, W. J. Evans, *Inorg. Chem.* **2010**, *49*, 10007–10012.

[2] For recent examples of guanidinate chemistry, see: a) C. Jones, C. Schulten, L. Fohlmeister, A. Stasch, K. S. Murray, B. Moubaraki, S. Kohl, M. Z. Ertem, L. Gagliardi, C. J. Cramer, *Chem. Eur. J.* **2011**, *17*, 1294–1303; b) J.-U. Rohde, W.-T. Lee, *J. Am. Chem. Soc.* **2009**, *131*, 9162–9163.

[3] For recent examples of β-diketiminate ($nacnac^-$) chemistry, see: a) M. M. Khusniyarov, E. Bill, T. Weyhermüller, E. Bothe, K. Wieghardt, *Angew. Chem. Int. Ed.* **2011**, *50*, 1652–1655; b) M. L. Scheuermann, U. Fekl, W. Kaminsky, K. I. Goldberg, *Organometallics* **2010**, *29*, 4749–4751; c) V. T. Annibale, L. M. Lund, D. Song, *Chem. Commun.* **2010**, *46*, 8261–8263.

[4] For recent examples of bis(phosphinimino)methanide chemistry, see: a) G. Ma, M. J. Ferguson, R. G. Cavell, *Chem. Commun.* **2010**, *46*, 5370–5372; b) A. Buchard, R. H. Platel, A. Auffrant, X. F. Le Goff, P. Le Floch, C. K. Williams, *Organometallics* **2010**, *29*, 2892–2900; c) S. Schulz, S. Gondzik, D. Schuchmann, U. Westphal, L. Dobrzycki, R. Boese, S. Harder, *Chem. Commun.* **2010**, *46*, 7757–7759.

[5] For recent examples of imidodiphosphinate chemistry, see: a) E. Ferentinos, D. Maganas, C. P. Raptopoulou, A. Terzis, V. Psycharis, N. Robertson, P. Kyritsis, *Dalton Trans.* **2011**, *40*, 169–180; b) T. Chivers, J. S. Ritch, S. D. Robertson, J. Konu, H. M. Tuononen, *Acc. Chem. Res.* **2010**, *43*, 1053–1062; c) D. Oyetunde, M. Afzaal, M. A. Vincent, I. H. Hillier, P. O'Brien, *Inorg. Chem.* **2011**, *50*, 2052–2054; d) S. D. Robertson, T. Chivers, J. Akhtar, M. Afzaal, P. O'Brien, *Dalton Trans.* **2008**, 7004–7011.

[6] a) S. E. Durran, M. R. J. Elsegood, S. R. Hammond, M. B. Smith, *Dalton Trans.* **2010**, *39*, 7136–7146; b) S. E. Durran, M. R. J. Elsegood, S. R. Hammond, M. B. Smith, *Inorg. Chem.* **2007**, *46*, 2755–2766; c) M. R. J. Elsegood, M. B. Smith, P. M. Staniland, *Inorg. Chem.* **2006**, *45*, 6761–6770.

[7] a) P. C. Kunz, C. Wetzel, M. Bongartz, A. L. Noffke, B. Spingler, *J. Organomet. Chem.* **2010**, *695*, 1891–1897; b) Z. García-Hernández, A. Flores-Parra, J. M. Grevy, A. Ramos-Organillo, R. Contreras, *Polyhedron* **2006**, *25*, 1662–1672; c) H. L. Milton, M. V. Wheatley, A. M. Z. Slawin, J. D. Woollins, *Inorg. Chim. Acta* **2005**, *358*, 1393–1400.

[8] a) S. Zhang, R. Pattacini, P. Braunstein, *Organometallics* **2010**, *29*, 6660–6667; b) W. Lackner-Warton, S. Tanaka, C. M. Standfest-Hauser, O. Öztopcu, J.-C. Hsieh, K. Mereiter, K. Kirchner, *Polyhedron* **2010**, *29*, 3097–3012; c) G. Margraf, R. Pattacini, A. Messaoudi, P. Braunstein, *Chem. Commun.* **2006**, 3098–3100.

[9] P. Bhattachararyya, A. M. Z. Slawin, M. B. Smith, *J. Chem. Soc., Dalton Trans.* **1998**, 2467–2475.

[10] V. V. Sushev, N. V. Belina, G. K. Fukin, Y. A. Kurskiy, A. N. Kornev, G. A. Abakumov, *Inorg. Chem.* **2008**, *47*, 2608–2612.

[11] A. Bondi, *J. Phys. Chem.* **1964**, *68*, 441–451.

[12] P. Gantzel, P. J. Walsh, *Inorg. Chem.* **1998**, *37*, 3450–3451.

[13] A. M. Z. Slawin, J. Ward, D. J. Williams, J. D. Woollins, *J. Chem. Soc., Chem. Commun.* **1994**, 421–422.

[14] a) Y.-L. Hsu, L.-C. Liang, *Organometallics* **2010**, *29*, 6201–6208; b) K. Izod, J. Young, W. Clegg, R. W. Harrington, *Dalton Trans.* **2005**, 1658–1663.

[15] a) M. Risto, J. Konu, T. Chivers, *Inorg. Chem.* **2011**, *50*, 406–408; b) J. D. Woollins, *J. Chem. Soc., Dalton Trans.* **1996**, 2893–2901.

[16] C. White, A. Yates, P. M. Maitlis, *Inorg. Synth.* **1992**, *29*, 228–234.

[17] M. A. Bennet, T. N. Huang, T. W. Matheson, A. R. Smith, *Inorg. Synth.* **1982**, *21*, 74–78.

[18] M. A. Bennet, A. K. Smith, *J. Chem. Soc., Dalton Trans.* **1974**, 233–241.

[19] W. Baratta, P. S. Pregosin, *Inorg. Chim. Acta* **1993**, *209*, 85–87.

[20] COLLECT Data Collection Software, R. Hooft, Nonius B. V. **1998**.

[21] DENZO: Z. Otwinowski, W. Minor, in *Methods in Enzymology, Macromolecular Crystallography, Part A, Vol. 276* (Eds.: C. W. Carter Jr., R. M. Sweet), Academic Press, **1997**, p. 307.

[22] SORTAV: R. H. Blessing, *Acta Crystallogr., Sect. A* **1995**, *51*, 33–38.

[23] a) R. H. Blessing, *J. Appl. Crystallogr.* **1997**, *30*, 421–426; b) DIRDIF-96: A Computer Program System for Crystal Structure Determination by Patterson Methods and Direct Methods Applied to Difference Structure Factors, P. T. Beurskens, G. Beurskens, W. P. Bosman, R. De Gelda, S. Garcia-Granda, R. O. Gould, R. Isräel, J. M. M. Smits, Crystallography Laboratory, University of Nijmegen, The Netherlands, **1996**.

[24] G. M. Sheldrick, *Acta Crystallogr., Sect. A* **2008**, *64*, 112–120.

Received: September 9, 2011
Published Online: January 9, 2012

